Aerospace Science and Technology 91 (2019) 434–441

Contents lists available at ScienceDirect

Aerospace Science and Technology

www.elsevier.com/locate/aescte

Enhanced bondline thickness analysis for non-rigid airframe structural assemblies

Pablo Coladas Mato [a], Philip Webb [a,*], Yigeng Xu [a], Daniel Graham [b], Andrew Portsmore [c], Edward Preston [b]

[a] School of Aerospace, Transport and Manufacturing, Cranfield University, College Road, Cranfield, Bedfordshire, MK43 0AL, UK
[b] GKN Aerospace UK, Golf Course Lane, Filton, Bristol, BS34 7QQ, UK
[c] GKN Aerospace UK, Falcon Yard, Ferry Road, Isle of Wight, PO32 6RA, UK

ARTICLE INFO

Article history:
Received 7 January 2019
Received in revised form 8 April 2019
Accepted 9 May 2019
Available online 13 May 2019

Keywords:
Non-rigid assembly
Bonded airframe structure
Bondline thickness
Adhesive flow
Direct linearization method
Quadratic programming

ABSTRACT

Adhesive bonding is a proven alternative to mechanical fasteners for structural assembly, offering lighter and thus more fuel efficient aircraft and cost-effective manufacturing processes. The effective application of bonded structural assemblies is however limited by the tight fit-up requirement, which is with sub-mm tolerance and can be a challenge for the industry to meet considering the variability of current part manufacturing methods and the conservative nature of the conventional tolerance stack-up analysis method. Such a challenge can discourage effective exploitation of bonding technologies, or lead to development of overengineered solutions for assurance. This paper addresses this challenge by presenting an enhanced bondline thickness variation analysis accounting for part deflection of a bonded skin-stringer assembly representing a typical non-rigid airframe structure. A semi-analytical model accounting for unilateral contact and simplified 1D adhesive flow has been developed to predict bondline thickness variation of the assembly under two typical curing conditions: namely autoclave curing and out-of-autoclave curing. The effects of component stiffness and manufacturing variations on bondline thickness are investigated by incorporating stringers of different stiffness, as well as shims of different thicknesses in-between the skin and stringer, in the stringer-skin assembly. A small-scale bonding demonstrator has been built and the physical results are in good agreement with the model prediction. It has been demonstrated that the part deflections need to be accounted for regarding fit-up requirement of bonded non-rigid structural assembly. The semi-analytical model offers more reliable and realistic prediction of bondline thickness when compared to a rigid tolerance stack-up. The analysis method presented can be a major technology enabler for faster, more economical development of the aircraft of the future, as well as of any analogue structures with high aspect ratios where weight savings and fatigue performance may be key objectives.

1. Introduction

The global aviation industry is experiencing steep growth; the UK's Aerospace Technology Institute, for example, forecasts a doubling in the number of commercial and business aircraft within the next two decades, with an associated asset value of several US$ trillion. This high-growth environment results in strong competition for market share and positioning; it creates a substantial incentive for technology improvements that may lead to improvements in manufacturing rate and efficiency, as well as increased energy efficiency or new functionalities [1].

Aircraft are manufactured as an assembly of a large number of parts, which are typically joined by means of mechanical fasteners such as rivets. With thousands of fasteners in each aircraft, this translates to a large weight added, as well as manufacture costs due to drilling and fastener insertion operations. It also leads to concerns over structural integrity due to stress concentration.

Adhesive bonding is a proven alternative to mechanical fastening which has found successful applications in the aerospace industry for decades. It can substantially cut manufacturing time and joint weight, in addition to other benefits such as preservation of the aerodynamic profile, improved mechanical and corrosion performance, and applicability to a multitude of different materials without needing large process changes. However, its industrial-

* Corresponding author.
E-mail addresses: p.coladas.mato@gmail.com (P. Coladas Mato), p.f.webb@cranfield.ac.uk (P. Webb), yigeng.xu@cranfield.ac.uk (Y. Xu), dan.graham@gknaerospace.com (D. Graham), andrew.portsmore@gknaerospace.com (A. Portsmore), ed.preston@gknaerospace.com (E. Preston).

https://doi.org/10.1016/j.ast.2019.05.024

ization has sometimes been limited due to difficulty in meeting quality requirements. Among these, bondline dimensional control is perceived as one important limiting factor which affects load distribution and joint strength [2,3].

Interface gap values resulting from tolerance stack-ups and dry-fit inspection typically exceed the maximum acceptable bondline thickness and permissible variation [4]. However, aircraft structural subcomponents are in most cases flexible (non-rigid); that is, assembly forces can cause deflections comparable to the geometrical tolerance values [5]. Thus, part flexibility can be capitalized on to mitigate manufacturing variation. This needs to be accounted for in the assembly tolerance analysis and requirement definition, as tolerances will otherwise be unnecessarily pessimistic. If a joining technology is perceived as too stringent, it may be wrongly discarded early during a development program, and the benefits and drawbacks of different manufacture and assembly concepts will not be properly assessed. This does not just apply to bonding, but also to greener alternatives to autoclave curing (AC) for application of the curing forces. For instance, out-of-autoclave (OoA) curing, which is less energy- and tooling-demanding than AC [6,7], also naturally offers less control over the final bondline geometry given the smaller forces applied; as a result, OoA may be sidelined early during bonding manufacturing development due to quality concerns, ultimately resulting in a more costly manufacture solution which may or may not be justified.

This observation on the relevance of part deflections for assembly tolerancing is not new: the effect has been known and utilized for decades in the aerospace [8–11] and automotive [12,13] sectors. It also has been incorporated into various inspection approaches [14–16] and commercial stochastic tolerancing software [17,18]. However, publicly available studies of the implications for bonding are strictly empirical [10]; meanwhile, Computer Aided Tolerancing (CAT) applications have focused largely on fastener- and spotweld-based assemblies. Quantitative study of the effect of part flexibility on bonding outcomes is, thus, left wanting for a reliable prediction tool accounting for continuous contact and adhesive flow characteristics.

This paper presents an enhanced bondline thickness variation analysis accounting for part deflection of a bonded skin-stringer assembly representing a typical non-rigid airframe structure. The background of the research is introduced in this section. The second section provides an overview of key aspects associated with the assembly variability management. The third section concerns the model setup, including an efficient algorithm solving the contact problem and simplified adhesive modeling. The fourth section presents a demonstrator assembly used for model verification. Results are compared to a FE model for in- and out-of-autoclave pressures, with varying component stiffness and in-built gap dimensions. General applicability of the model is discussed. The last section summarizes the main findings of the research and a way forward for further work.

2. Key aspects with assembly variability management

2.1. Recorded aerostructural bonding issues

The problem of achieving a good adherend fit is well documented; for example, industry communications in the 1950s to 1970s highlighted the need for appropriate tooling to push parts together, with stringent tolerances which may not be met by hard tooling [9,19,20]. The Primary Adhesively Bonded Structures Technology (PABST) program, undertaken by McDonnell Douglas during the 1970s, highlighted how not even autoclave and flexible bags may enable a proper fit, and how tooling concepts can make all the difference by facilitating deflection of different adherends [10]. Later reflections on this programme, and application of its learnings to Fokker and SAAB products, emphasized the need to account for deflection of the adherends and how the parts themselves, rather than the tooling, determine the final geometry [11,21]. Although geometric tolerances were quoted following the PABST development, no calculation method, nor any systematic testing approach to ascertain the geometric capability of the bonding process, were reported.

2.2. Modeling of adhesive flow

Though it may be tempting to assume hot-setting adhesives flow freely and fully accommodate any part deflection, this is not strictly true. This is for two reasons: first, adhesives will usually contain a medium, such as a carrier film or glass beads, which effectively behaves as incompressible, thus limiting the minimum distance between adherends. Secondly, viscous resistance to flow increases sharply as the adhesive layer is squeezed and becomes thinner; thus, even under large pressures, adhesive flow is limited and the bondline thickness becomes stable before the cure is complete. This slow flow of the viscous adhesive under pressure is known as squeeze flow.

Squeeze flow modeling in planar bondlines has not been widely documented for dominantly-viscous materials. Industry reports tend to characterize the bondline geometry empirically or neglect adhesive flow mechanics when discussing tolerances [9,10,19,20,22]. It has received some limited attention to assess how different parameters help control bondline thickness [23], although without any consideration for adherend behavior. Squeeze flow also has been studied in cases where the focus was not bondline thickness, but other quality criteria such as void formation [24]. The packaging industry has seen more recent study to support process parameter optimization [25], though with a focus on excess material and cycle time. In all three cases referenced, a one-dimensional viscous flow model was used, justified by the high aspect ratio of the bonded joint, achieving good agreement with experimental results.

2.3. Non-rigid assembly modeling

Although knowledge of the impact of part deflections has been formalized at least for 4 decades [12], it is only close to the new millennium that this is actively studied and incorporated into models, driven by an increasing push for manufacturing efficiency and expanding computational capacity. The Association for the Development of Computer-Aided Tolerancing Systems (ADCATS) research group developed simplified approaches to modeling of part variation and part compliance using superelements and spectral decomposition, and showed their application to fastened assemblies assuming perfect fit at joined nodes [26,27]. The Stream-of-Variation method, incorporated considerations of how assembled parts are deformed to fit each other and mitigate location errors [28], though without further considerations of part contact outside joined spots or deflection due to tooling variation [29]. The Method of Influence Coefficients (MIC) was developed as a linear expansion of variation accounting for part deformation within a PCFR cycle (Position-Clamp-Fasten-Release), by considering only the joined nodes and thus reducing computation time dramatically. The RDnT software for stochastic assembly tolerancing was expanded with a non-rigid module [17], including the potential to account for contact, as was the similar 3DCS [18,30]. The effect of contact between non-joined points was also incorporated to the MIC-based calculation, showing considerable influence in the final simulation results, and highlighting difficulties with modeling and prediction of friction-based interactions [31–34].

These methods have been primarily applied to automotive assemblies or generic sheet metal. However, in the past decade aerospace-type assemblies have also been studied, for example, with application and second-order expansion of MIC for fastened fuselage frames [35]; use of 3DCS for analysis of wing spar-panel fastening [36]; and optimization of fuselage panel skin-stringer temporary fastener positioning, using iterative compliance matrix updating without [8] and with contact considerations [37].

It has been noted that most studies of assembly variation do not dwell on the joint formation itself. In most cases, two nodes are simply joined by a fastener or spot weld. In some work, the thickness of a weld nugget [38], the dimensions of a hole and rivet [35], and the deformation caused by the fastener insertion [39], have been added into the assembly model, although in these cases the part clearance was always assumed to be zero at the joined spot.

Study of fillet welding [40,41] showed that not only can the joint formation mechanics be a contributor to variability, but also that variation of the individual parts assembled can amplify the variation substantially even when dealing with simple geometries. Thus, formation of the joint and variation of the assembly details should be studied together. It is worth underscoring that these welded joints were not assumed to have zero thickness; indeed, variation was implemented as a change in the joint geometry. This rings close to the case of an adhesively bonded joint where no two points can be assumed to be brought in contact, and the bondline thickness is likely to vary throughout.

3. Model setup

3.1. Basic features of the model

Before enunciating the technical detail of the modeling approach, it is worth highlighting the basic features of the model, which are different to the ones commonly found in the literature.

First, the external forces applied are known as the assembly in the current study is vacuum bagged and oven or autoclave cured; the clamping or fastening forces for the joints in literature would be a product of the part deviation from nominal and are normally unknown beforehand.

Second, the focus in this study is not the assembly deformation after release of the assembly forces due to part deformations and internal stresses. Rather, it is the joint geometry (namely, the bondline thickness) that is key. This would typically be prescribed as zero in fastening or spotwelding applications, and as a product of the initial deviations in fillet welding. Meanwhile, in the current model it is an unknown. In addition, since the joint geometry is the quantity of interest, the calculation finishes at the joint formation (adhesive cure) step and therefore the springback is not considered.

Fig. 1 illustrates the formation of the bondline thickness of uncured bonded joint. The bondline thickness of the joint will be determined by two separate mechanisms: the ability of adhesive to flow, and the deflection of the adherends. Both of which are driven by the external pressure. Since the adhesive's flow resistance is highest when the bondline is thinnest, the external pressure will be reacted where the adherends are brought closest together. Thus, the bondline thickness is separated into two components: a wet component for minimum bondline thickness and a dry component for adherend separation left after discounting the wet component.

The interaction between adherends prior to the formation of the bonded joint, which consists of the transmission of pressure through the uncured adhesive, is approximated as a contact interaction at the regions of lowest adhesive thickness, since these are where the adhesive resists flow the most and becomes highly pressurized. Thus, the "dry" component is approximated as the clearance between the adherends when pushed against each other as shown in Fig. 1.

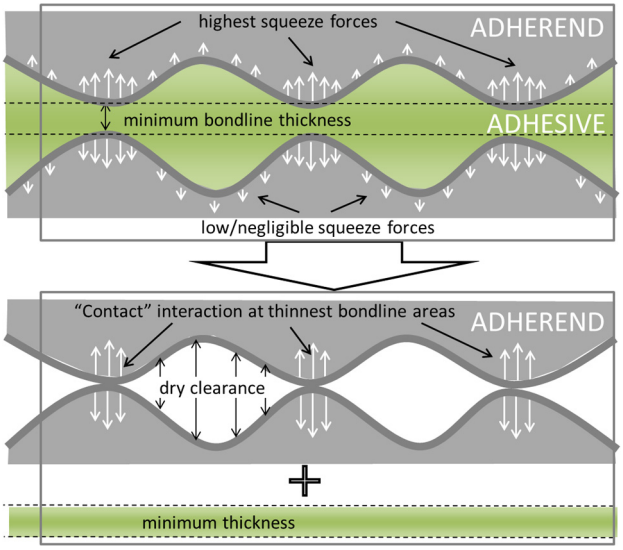

Fig. 1. Separation of the uncured bonded joint into dry and wet components.

3.2. Wet component: minimum bondline thickness

Flow of the adhesive at the thinnest bondlines was modeled as one-dimensional squeeze flow (1DSF), as in references [23–25].

The basic assumptions are:

(a) The uncured adhesive behaves as a Newtonian fluid.

(b) Each layer of fabric acts as a solid boundary and the layers of adhesive under and above it act as different flow domains.

(c) Both adherends can be approximated as flat and parallel for flow purposes.

(d) The problem is quasi-steady, and thus effects of inertia and accelerations are negligible (quasi-static force equilibrium applies).

(e) Flow only takes place in the cross-section plane without any longitudinal component.

(f) Adhesive flows freely once squeezed out from the space between adherends.

The general concept and dimensions are captured in Fig. 2. Thickness of a single squeezed bondline can be idealized [23] as

$$b_{1t}(t, Z_0) = \frac{1}{\sqrt{\left(\int_0^t \eta^{-1}\mathrm{d}t\right)\frac{2P}{w^2} + \frac{1}{Z_0^2}}} \tag{1}$$

where η is the adhesive kinematic viscosity, $P = P_{external} - P_0$ the manometric pressure applied, $Z_0 = b_{1t}\ (t = 0)$ the initial bondline thickness, and w the bond width. The width of the bondline is assumed to remain constant and equal to w at all times.

The total bondline thickness for n layers of film adhesive with carrier will thus be

$$b_{bond} = \sum_{j=1}^{j=n+1} b_{1t}\left(t, Z_{0_j}\right) + \sum_{k=1}^{k=n} b_{carrier_k} \tag{2}$$

The only term dependent on the adhesive properties, as seen in Eq. (1), is $\left(\int_0^t \eta^{-1}\mathrm{d}t\right)$ which is a function of the rheology curve for the specific temperature cycle encountered. The evolution of the viscosity with time is highly dependent on the heat rate [42], which can be difficult to predict and control for industrial equipment and large assemblies, and even idealized test data is not always provided by suppliers. For the current study, this information is estimated based on the data in literature and experimentally observed minimum bond thickness.

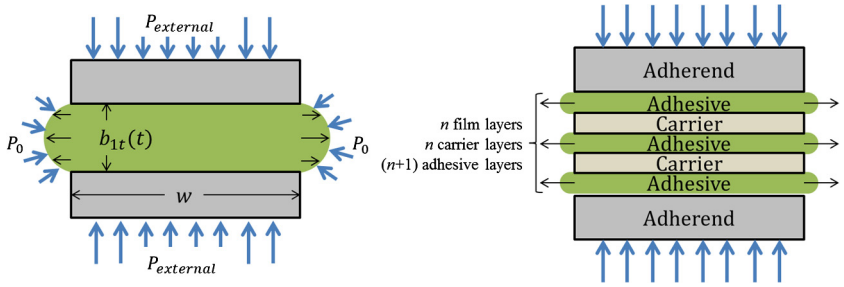

Fig. 2. Squeeze-flow with a single domain (left) and multiple domains (right).

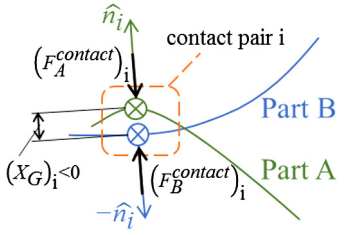

Fig. 3. Part interaction based on node pairs with normal reactions only.

3.3. Dry component: clearance from part shape mismatch

The dry assembly has been modeled by part linearization and modeling of the hard contact into a quadratic equation. The contact solution follows the prior art in [43], with the node interactions reframed to better reflect the assumptions of the bonding problem. The solution is reformulated below for the reader's benefit. Solution of the contact problem starts with the following simplifications:

1. The individual assembly parts satisfy the small deformations hypothesis, which justifies the application of the principle of superposition;
2. External forces are applied normal to the nominal surface at each position;
3. Adhesive behavior has been accounted for in the wet component (as presented in Fig. 1) and will be ignored for the determination of the dry component of the bondline thickness. The adhesive will however transmit the reaction forces and act as a lubricant which eliminates any friction between parts from tangential displacements.

Based on the assumptions above, only the interactions normal to the nominal mating surface (that is, only normal forces and displacements) are considered, as represented in Fig. 3. Thus at node i,

$$\boldsymbol{F_i} = (F_{i,x}, F_{i,y}, F_{i,z}) \cdot \hat{n}_i \tag{3}$$

$$\boldsymbol{X_i} = (X_{i,x}, X_{i,y}, X_{i,z}) \cdot \hat{n}_i \tag{4}$$

A linear model is constructed based on the compliance matrix:

$$\Delta X = \begin{bmatrix} \Delta X_1 \\ \vdots \\ \Delta X_N \end{bmatrix} = \begin{bmatrix} U_1 & \cdots & U_{1N} \\ \vdots & \ddots & \vdots \\ U_{N1} & \cdots & U_{NN} \end{bmatrix} \begin{bmatrix} F_1 \\ \vdots \\ F_N \end{bmatrix} = \boldsymbol{U} F \tag{5}$$

The problem only needs to concern itself with the nodes at interfaces; thus, the compliance matrix is obtained by applying a unit force in a finite element mesh and recording the deflections at each point of interest.

The contact problem is formulated by considering the points interfacing between two linearized bodies A, B. The gap between them is also linearized, and a single normal $\hat{n}_i$ is picked at each contact pair such that $(X_G)_i = (X_B^A - X_A^B)_i > 0$ when there is clearance.

$$\Delta X_G = \Delta X_B^A - \Delta X_A^B = \boldsymbol{U_B^A} F_B - \boldsymbol{U_A^B} F_A \tag{6}$$

Consider deflection due to internal forces that arise due to contact, these will be applied on both parts, due to action-reaction:

$$\left(F_B^{contact}\right)_i = -\left(F_A^{contact}\right)_i = \left(F^{contact}\right)_i \cdot \hat{n}_i \tag{7}$$

$$\Delta X_G = \Delta X_B^A - \Delta X_A^B = \boldsymbol{U_B^A} F_B^{external} - \boldsymbol{U_A^B} F_A^{external} + \left(\boldsymbol{U_B^A} + \boldsymbol{U_A^B}\right) F^{contact} \tag{8}$$

Considering computational implementation, this effectively means that the forces are being applied sequentially, as $F^{contact}$ is initially unknown:

$$\Delta X_G = \left[\left(\Delta X_B^{initial} - \Delta X_A^{initial}\right) + \boldsymbol{U_B^A} a F_B^{external} - \boldsymbol{U_A^B} F_A^{external}\right] + \left(\boldsymbol{U_B^A} + \boldsymbol{U_A^B}\right) F^{contact} = X_G^{no\ contact} + \boldsymbol{U_G} F^{contact} \tag{9}$$

The unilateral contact condition is enforced by quadratic programming, by solving a problem resulting from the Hertz-Signorini-Moureau criteria [43,44].

1. $(X_G)_i \geq 0, \quad \forall i$ – no penetration (10)
2. $\left(F^{contact}\right)_i \geq 0, \quad \forall i$ – no "pull" reaction during cure (11)

From Eqs. (10), (11) and as X_G, $F^{contact}$ are column vectors of positive values,

$$(X_G)^{\mathrm{T}} F^{contact} \geq 0 \tag{12}$$

The definition of X_G in Eq. (9) is substituted in Eq. (12):

$$\left(X_G^{no\ contact}\right)^{\mathrm{T}} F^{contact} + \left(F^{contact}\right)^{\mathrm{T}} \boldsymbol{U_G} F^{contact} \geq 0 \tag{13}$$

Further, either the contact force or the gap will be zero at each contact pair, which is expressed by the third Hertz-Signorini-Moureau criterion:

3. $(X_G)_i \left(F^{contact}\right)_i = 0, \quad \forall i$ (14)

Thus, the quadratic inequation (13) can be turned into a convex minimization problem which looks for

$$\operatorname{argmin}(f) = \operatorname{argmin}\left(\left(X_G^{no\ contact}\right)^{\mathrm{T}} F^{contact} + \left(F^{contact}\right)^{\mathrm{T}} \boldsymbol{U_G} F^{contact}\right) \tag{15}$$

where $F^{contact}$ is the N-dimensional dependent variable.

In this implementation, the problem has been solved using MATLAB's quadprog (QP) function, which offers pre- and post-processing for increased efficiency, algorithm selection, and convergence parameter control with little user effort.

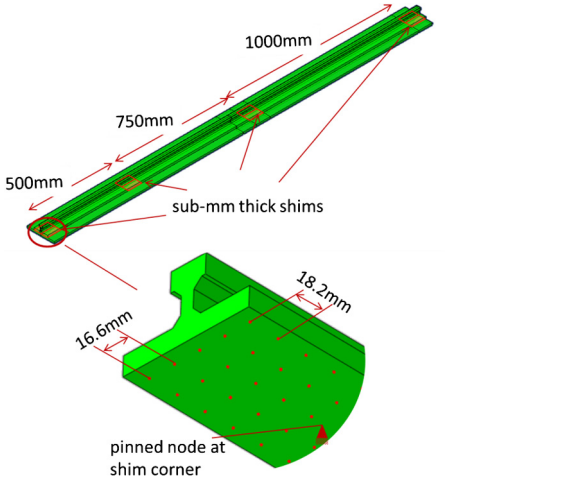

Fig. 4. Assembly and subset of nodes considered for verification against FEA.

The problem is reformulated for input to the function as

$$f = \frac{1}{2}\left(F^{contact}\right)^{\mathrm{T}} 2\boldsymbol{U_G} F^{contact} + \left(X_G^{no\ contact}\right)^{\mathrm{T}} F^{contact},$$
$$\begin{cases} -\boldsymbol{U_G} F^{contact} \leq X_G^{no\ contact} \\ (0)_{N\times 1} \leq F^{contact} \end{cases} \tag{16}$$

And the input to MATLAB is (with each variable/parameter appearing in the same order):
`F_contact = quadprog (2*U_G, X_G_nocontact, -U_G, X_G_nocontact, [],[],zeros(N,1),[])`
with the `[]` empty square brackets denoting lack of equality constraints or upper bounds.

The algorithm used to determine the contact force of the problem was quadprog's default interior-point convex optimization algorithm.

From the resulting value of $F^{contact}$, it is straightforward to calculate the individual part positions, as well as X_G which is the parameter of most interest in this study.

4. Results and discussion

4.1. Stringer-skin assembly for model validation

The model proposed in Section 3 will first be validated against the FEA results of a stringer-skin assembly. A bonding scenario with variation occurring over multiple ranges has been used for validation. This consists of a thin (5 mm) flat skin plate, and flat stringers bonded on top of it. Stringer profile variation was emulated by introducing shims of controlled thickness at variable intervals (Fig. 4).

A physical assembly demonstrator has been manufactured for this study. The skin plates were gap checked against the table prior to bonding using a 0.05 mm feeler gauge, with no gaps detected. Given the skin flatness and high stiffness of the bonding table used, the skin was modeled as an encastred plate, and the shims as padups integral to it.

The stringer is of a constant cross-section and both parts were made of representative aluminum alloy ($E = 72000$ MPa, $\nu = 0.30$). Two cross-sections were considered: 'Thick' ($I_z \approx 275000$ mm^4 with a 12 mm-thick foot flange) and 'Thin' ($I_z \approx 120000$ mm^4 with a 4 mm-thick foot flange).

4.2. Dry model validation against FEA results

As a first verification of the semi-analytical model, comparison was established with results from conventional Finite Element Analysis (FEA) with Abaqus. No adhesive was considered in this case as the focus of the verification was on part deflection and contact enforcement (dry part). This also had the effect of increasing the maximum deflection achievable, and thus improving detectability of deviations.

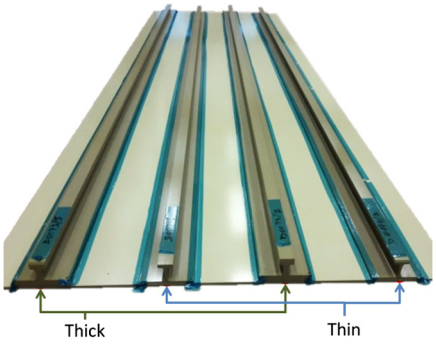

Fig. 5. Test panel with both 'Thick' and 'Thin' stringers.

Results for deflection were obtained for two models in each case: FEA with a fine solid mesh (C3D8 elements), and the proposed QP-based method using a stringer compliance matrix obtained from the same mesh.

For the QP model, each stringer was reduced to $128 \times 5 = 640$ nodes equidistant on the foot (Fig. 4), with matching nodes on the skin and shims. By assuming the skin panel to be perfectly flat and the table infinitely stiff, the need to model the assembly jointly (including skin-tool contact and impact of one stringer on the rest of the panel) was effectively removed. Thus, each stringer's deflection was modeled separately. This resulted in much smaller matrices and faster calculation times.

The results were extracted for nodes in the middle of the stringer flange and 1/10 the flange width from the edge. A small subset of the results (0.5 mm shim with the highest and lowest pressures) is shown in Fig. 6; there is very good agreement between the FEA and QP results (solid and dashed lines), except for moderate deviations in the deflection achieved where there is no adherend contact in a span between shims, as well as for the foot flange edge (red lines) of the 'Thin' stringers.

The root-mean-square (RMS) difference between the QP and FEA results generally stay below 5% of the initial gap as shown in Fig. 5. The only substantial divergence was when dealing with a thin foot flange; in this case, the failure of the coarse node grid to properly account for the stringer edges resulted in inaccurate modeling of the contact interactions, and flange deflection was overestimated ("edge" red lines in Fig. 7). This can be easily improved by adding more nodes in the width of the stringer flange, demonstrating the validity of the proposed semi-analytical model.

4.3. Physical test results and reliability of flow modeling assumption

The dry component simulation of the proposed model has shown good agreement with FEA results. The remaining work is to verify that the adhesive flow assumptions hold satisfactorily, which will be tested with the physical assembly demonstrator shown in Fig. 4. The intention of this test is not to verify the exact minimum-bondline-thickness achieved. Rather, the objective is to validate the model simplification presented in Section 3, where adhesive behavior is only relevant for calculation of a minimum bondline thickness (wet component). If this is the case, it is reasonable to use 1DSF, and ($\int_0^t \eta^{-1} dt$), along with the other film parameters, can then be calculated through material characterization (e.g. using a rheometer as in [42]), or the expected minimum-bondline-thickness can be determined though process-specific tests that replicate the pressure and thermal cycle. In

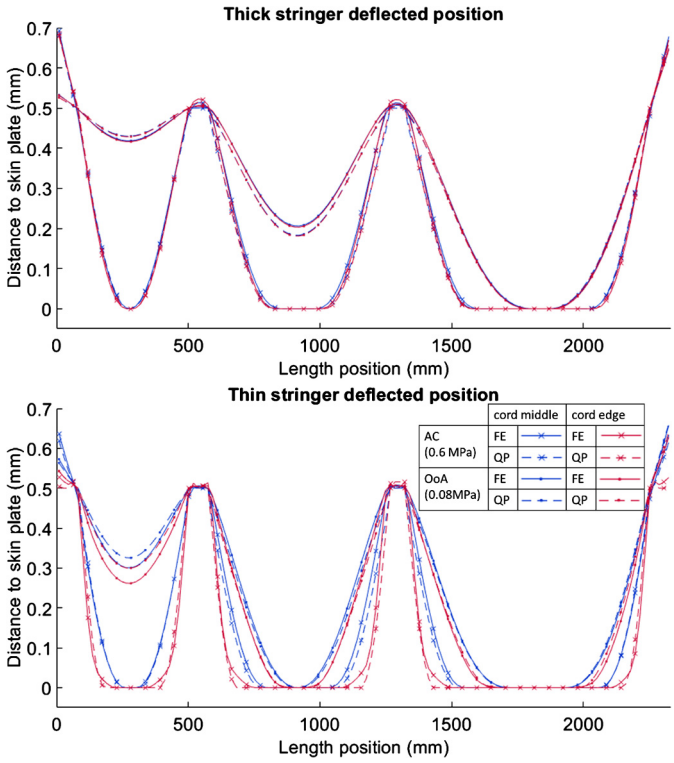

Fig. 6. Part deflections as obtained by FEA and by the proposed method, for 0.5 mm gaps with no adhesive, under the maximum and minimum pressures considered. (For interpretation of the colors in the figure(s), the reader is referred to the web version of this article.)

either case, one should confirm the actual thermal cycle in the joint, especially in large assemblies where the part and tooling's thermal mass may result in large deviations across the structure and from the nominal. Usual industry practice includes attachment of multiple thermocouples to ensure the structure has undergone the correct treatment. Closer scrutiny of the adhesive model and properties may be in order if other outcomes, such as spew fillet volume and void formation, are also of concern.

The tests used the same skin-shims-stringers arrangement presented above, but incorporating adhesive outside the shimmed areas. Trials were conducted with 1 and 2 adhesive film layers.

The bonded assemblies were simulated with the QP model as described above. For the minimum bondline thickness, constant viscosity $\eta = 50$ Pa s, total squeeze time $t = 1200$ s, initial per-layer thickness $Z_0 = 0.1$ mm, and carrier thickness $b_{carrier} = 0.050$ mm was assumed. With $X_0 = 83$ mm, this results in minimum thickness values in the 0.081 mm and 0.146 mm for 1 and 2 layers, respectively.

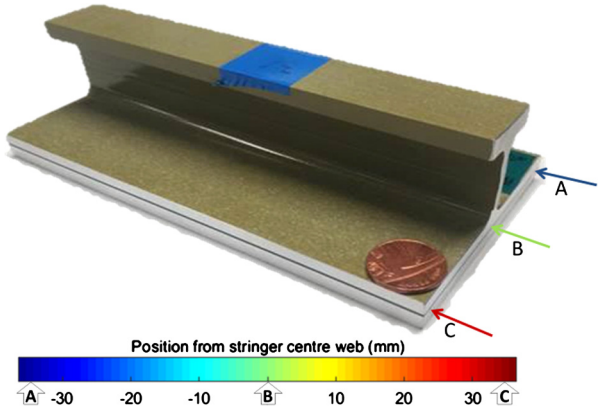

Fig. 8. Section taken from a 'Thin' stringer, with microscopy locations marked and a penny for scale.

The assembly comprised a skin plate with two 'thick' and two 'thin' stringers, one of each with 0.2 mm shims (1 film layer) and other with 0.3 mm shims (2 film layers). The number of layers is the maximum that would not overfill the artificial gaps according to manufacturing best practice, based on a nominal cured layer thickness of 0.125 mm. The parts were bonded using an epoxy adhesive with scrim carrier (Cytec FM94-0.06K). The assembly was encapsulated in a vacuum bag and cured at a representative autoclave pressure of 0.6 MPa. The heat cycle comprised heating at a 2 °C/min rate, holding at 120 °C for an hour.

The stringers were machined to a tight profile tolerance of 0.2 mm in the bonding surface. Simulation of assembly for parts with such small variation were found yield minimal (<25 µm) deviations from nominal, so the results from assembling nominally-flat stringers were used instead of individual part inspection values.

The cured assemblies were sectioned into ~200 mm segments at regular intervals between the shims, at locations adjacent to the shims and where minimum bondline thickness was expected. The bondline thickness was assessed via optical microscopy, with three spots measured at each cross-section (Fig. 8). The longitudinal section distribution is presented in Fig. 9, along with example results (simulated and measured for 'Thick' stringers).

The results show consistent behavior of the adhesive under each stringer at high pressures, with small variability among the measured thicknesses, with standard deviations below 0.020 mm and numerical results in the range of the 1DSF preliminary sizing (Table 1). However, there exist divergences between stringers which are likely not fully explained by slight differences in effective heat rates, with the thin stringers obtaining more variable bondlines.

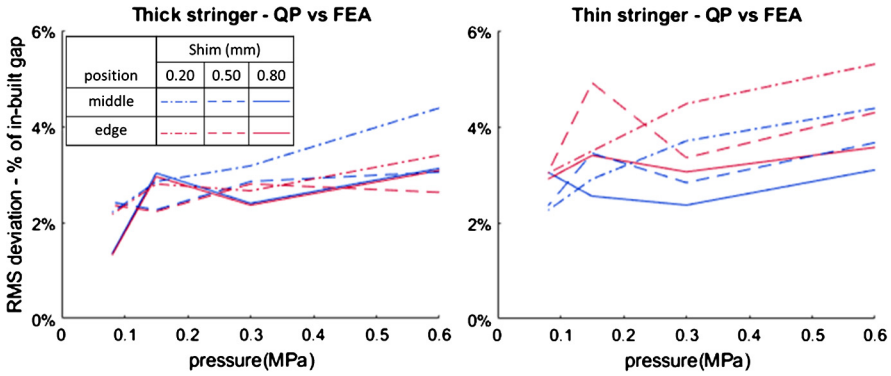

Fig. 7. RMS deviation between all QP and FEA simulations performed (dry component only).

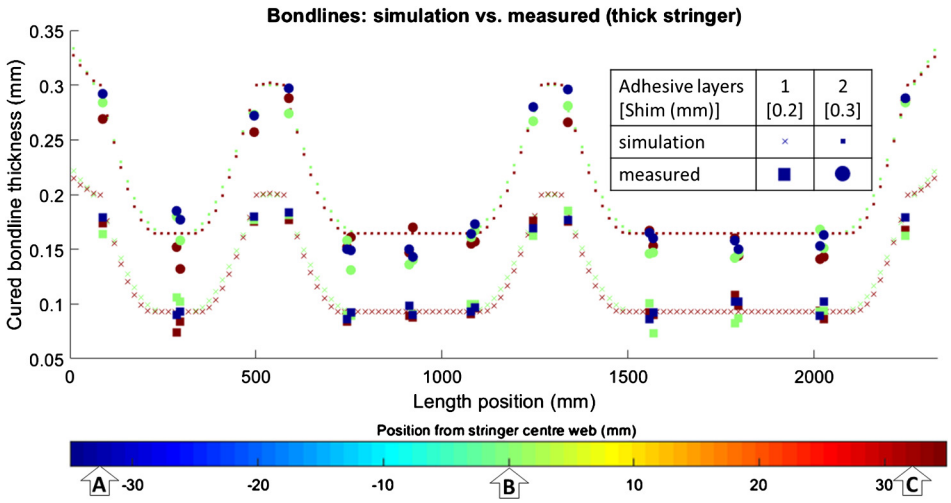

Fig. 9. Predicted and measured (small and large markers, respectively) bondline thicknesses for the 'Thick' stringers under 0.6 MPa. The section measurements show good agreement with the predicted results.

Table 1
Measured minimum bondline thicknesses: standard deviation and root mean square (RMS) difference to the 1DSF prediction.

Adhesive layers [Shim (mm)]	'Thick' stringer		'Thin' stringer	
	σ (mm)	RMS (mm)	σ (mm)	RMS (mm)
1 [0.2]	0.007	0.008	0.012	0.024
2 [0.3]	0.012	0.016	0.018	0.023

5. Conclusions

The model provides a good approximation of the demonstrator stringer behavior for a representative scenario, when compared with a more resource-intensive FEA simulation from a commercial package. The Matlab-based solution provides a better understanding of the development of bondline geometries and is easily shared across an organization. It allows easy integration and experimentation with multiple data sources or additional post-treatment. This solution should also be possible to integrate in existing CAT packages that calculate parts' elastic behavior with contact, provided surface-based force application and variable-size joint elements (for representation of the adhesive joint) are supported; such integration would also benefit from the ability to input part shape variation, monitor distances between surfaces at multiple points, and measure initial surface dimensions such that a potential violation of the adhesive flow assumptions may be flagged up.

The proposed method offers considerable advantages against a simple tolerance stack for non-rigid simple assemblies, owing to its ability to achieve less conservative bondline predictions by accounting for part deflection and adhesive flow. The implementation has been found to offer satisfactory predictive capability, taking into account typical product tolerances and measurement uncertainties. With this tool, it is possible to evaluate diverse assembly concepts and make better-informed tolerance-allocation decisions for bonded assemblies of monolithic parts.

The importance of adhesive contribution to geometrical variation, and the potentially-critical role of the bonding procedure, has been highlighted both with model and physical test article results. Furthermore, the simulations carried out highlight the interaction of thin stringer flanges with interface steps, resulting in deformations where stringer cross-sections experience changes in shape. The experimental work also points out to a natural limitation of the dry-wet separation which manifests itself when adherends are thin enough; the cross-section deforms under the external and adhesive forces, changing the shape of the adhesive flow domain. This effect can place an inherent limitation on modeling accuracy for assemblies of sheet stringers or doublers. Inaccuracies (not observed here) may likewise arise in assemblies where part twist is significant, making the flow asymmetrical in each cross-section; or when gaps are locally large enough that some flow may happen through the length of the stringer. In this light, laminate or doubly-curved structures may especially benefit from method refinement.

The next stage of development will be the study of bonded assemblies where the part itself causes the bondline variability, as well as physical OoA rather than AC curing, testing different boundary conditions, and removing the assumption of perfect, stiff skins.

Further development should also look at applicability to larger, more-representative assemblies. This includes factors such as doubly-curved geometries and large (several mm) deformations which may be unsuitable for linear modeling. The scope of applicability will need to be fully explored before it is possible to make a leap to wide industrialization; however, the initial results show encouraging capability for simple geometries. The semi-analytical model presented herein offers more reliable and realistic prediction of bondline thickness; as such, it can be a major technology enabler for lighter and more cost-effective development of high-performance structures. The scope of applicability is likely to extend beyond aerospace; additional opportunities for application may be found in other stiffened thin-walled structures, such as marine or automotive, which stand to benefit substantially from the weight savings, performance improvements, and corrosion resistance offered by adhesive bonding. Some of the modeling assumptions, especially around adhesive flow and force application, may need to be examined for these cases. For now, the technique presented offers tempting possibilities to support development of airframes of the near future.

Declaration of Competing Interest

There is no competing interest.

References

[1] ATI, Raising Ambition: Technology Strategy and Portfolio Update 2016, https://www.ati.org.uk/wp-content/uploads/2017/10/Raising-Ambition-ATI-Technology-Strategy-Portfolio-Update-2016.pdf, 2016. (Accessed 18 December 2018).

[2] J. Tomblin, K. Strole, G. Dodosh, L. Ilcewicz, Assessment of Industry Practices for Aircraft Bonded Joints and Structures, FAA report DOT/FAA/

AR-05/13, 2005, http://www.tc.faa.gov/its/worldpac/techrpt/ar0513.pdf. (Accessed 2 March 2016).
[3] L.J. Hart-Smith, Adhesive Layer Thickness and Porosity Criteria for Bonded Joints, USAF contract report AFWAL-TR-82-4172, Long Beach, California, https://apps.dtic.mil/dtic/tr/fulltext/u2/a129817.pdf, 1982. (Accessed 2 March 2016).
[4] L.J. Hart-Smith, Adhesively bonded joints in aircraft structures, in: L.F.M. da Silva, A. Öchsner, R.D. Adams (Eds.), Handb. Adhes. Technol., Heidelberg, 2011, pp. 1104–1147.
[5] G.N. Abenhaim, A. Desrochers, A. Tahan, Nonrigid parts' specification and inspection methods: notions, challenges, and recent advancements, Int. J. Adv. Manuf. Technol. 63 (2012) 741–752, https://doi.org/10.1007/s00170-012-3929-2.
[6] H. Nobis, W. Roeglin, O. Bischoff, A. Schroeder, Method for autoclave-free adhesive bonding of components for aircraft, 2010, Patent EP1984241 (B1).
[7] T. Centea, L.K. Grunenfelder, S.R. Nutt, A review of out-of-autoclave prepregs – material properties, process phenomena, and manufacturing considerations, Composites, Part A 70 (2015) 132–154, https://doi.org/10.1016/j.compositesa.2014.09.029.
[8] G. Liu, W. Tang, Y.-L. Ke, Q.-L. Chen, Y. Bi, Modeling of fast pre-joining processes optimization for skin-stringer panels, Assem. Autom. 34 (2014) 323–332, https://doi.org/10.1108/AA-05-2014-036.
[9] Conference on bonded aircraft structures, Aircr. Eng. Aerosp. Technol. 29 (1957) 139–142, https://doi.org/10.1108/eb032825.
[10] K.L. Land, F.B. Lennert, Primary Adhesively Bonded Structure Technology (PABST). Phase III: Tooling, Fabrication and Quality Assurance, USAF report AFFDL-TR-79-3154, 1979.
[11] L.J. Hart-Smith, G. Strindberg, Developments in adhesively bonding the wings of the SAAB 340 and 2000 aircraft, Proc. Inst. Mech. Eng., G J. Aerosp. Eng. 211 (1997) 133–156, https://doi.org/10.1243/0954410971532578.
[12] N. Takezawa, An improved method for establishing the process-wise quality standard, JUSE Reports Stat. Appl. Res. 27 (1980) 63–76.
[13] S.C. Liu, S.J. Hu, Variation simulation for deformable sheet metal assemblies using finite element methods, J. Manuf. Sci. Eng. 119 (1997) 368–374.
[14] P. Hammett, J. Baron, D. Smith, Automotive Body Measurement System Capability, Auto/Steel Partnership report, Southfield, http://www-personal.umich.edu/~phammett/Papers/asp-meas-rept.PDF, 1999. (Accessed 5 May 2016).
[15] H. Radvar-Esfahlan, S.-A. Tahan, Nonrigid geometric metrology using generalized numerical inspection fixtures, Precis. Eng. 36 (2012) 1–9, https://doi.org/10.1016/j.precisioneng.2011.07.002.
[16] F. Thiébaut, C. Lacroix, C. Lartigue, L. Andolfatto, Evaluation of the shape deviation of non rigid parts from optical measurements, Int. J. Adv. Manuf. Technol. 88 (2017) 1937–1944, https://doi.org/10.1007/s00170-016-8899-3.
[17] R. Söderberg, L. Lindkvist, S. Dahlström, Computer-aided robustness analysis for compliant assemblies, J. Eng. Des. 17 (2006) 411–428, https://doi.org/10.1080/09544820500275800.
[18] DCS, 3DCS Mechanical Solutions, https://www.cenit.com/fileadmin/dam/3DS-PLM/PDFs/3DCS_Mechanical_Variation_Analyst.pdf, 2013.
[19] W.E. Goff, Methods of airframe production, Flight Int. (1973) 873–874.
[20] E.J. Catchpole, Development of synthetic resin adhesives: a review of the background to adhesives for metal-to-metal bonding and honeycomb sandwich construction and their current scale of application, Aircr. Eng. Aerosp. Technol. 35 (1963) 7–19, https://doi.org/10.1108/eb033669.
[21] L.J. Hart-Smith, Adhesive bonding of aircraft primary structures, SAE Transact. 89 (1980) 3718–3782, https://doi.org/10.4271/801209.
[22] P. Hubert, A. Poursartip, A review of flow and compaction modelling relevant to thermoset matrix laminate processing, J. Reinf. Plast. Compos. 17 (1998) 286–318.
[23] A.J. Smiley, M. Chao, J.W. Gillespie Jr., Influence and control of bondline thickness in fusion bonded joints of thermoplastic composites, Compos. Struct. 2 (1991) 223–232.
[24] R.J. Chester, J.D. Roberts, Void minimization in adhesive joints, Int. J. Adhes. Adhes. 9 (1989) 129–138.
[25] B.A. Morris, J.M. Scherer, Modeling and experimental analysis of squeeze flow of sealant during hot bar sealing and methods of preventing squeeze-out, J. Plast. Film Sheeting 32 (2016) 34–55, https://doi.org/10.1177/8756087915578183.
[26] K.G. Merkley, Tolerance Analysis of Compliant Assemblies, PhD Thesis, Brigham Young University, 1998.
[27] B.F. Bihlmaier, Tolerance Analysis of Flexible Assemblies Using Finite Element and Spectral Analysis, MSc Thesis, Brigham Young University, 1999.
[28] S.J. Hu, Stream-of-variation theory for automotive body assembly, CIRP Ann. 46 (1997).
[29] J.V. Abellán Nebot, Prediction and Improvement of Part Quality in Multi-Station Machining Systems Applying the Stream of Variation Model, PhD Thesis, Universitat Jaume I, 2011.
[30] DCS, 3DCS FEA Compliant Modeler, www.plmmarketplace.com/upload/3DCS_FEA_Compliant_Modeler_Overview_2.ppt, 2007. (Accessed 10 October 2016).
[31] S. Dahlström, L. Lindkvist, Variation simulation of sheet metal assemblies using the method of influence coefficients with contact modeling, J. Manuf. Sci. Eng. 129 (2007) 615–622, https://doi.org/10.1115/1.2714570.
[32] L. Lindkvist, K. Wärmefjord, R. Söderberg, Tolerance simulation of compliant sheet metal assemblies using automatic node-based contact detection, in: Proc. IMECE2008 2008 ASME Int. Mech. Eng. Congr. Expo., Oct. 31-November 6, 2008, Boston, Massachusetts, USA, 2008.
[33] X. Liao, G.G. Wang, Non-linear dimensional variation analysis for sheet metal assemblies by contact modeling, Finite Elem. Anal. Des. 44 (2007) 34–44, https://doi.org/10.1016/j.finel.2007.08.009.
[34] B. Lindau, K. Wärmefjord, L. Lindkvist, R. Söderberg, Aspects of fixture clamp modeling in non-rigid variation simulation of sheet metal assemblies, in: Proc. ASME 2013 Int. Mech. Eng. Congr. Expo., San Diego, California, USA, 2013.
[35] A. Stricher, Tolérancement flexible d'assemblages de grandes structures aéronautiques, PhD Thesis, École normale supérieure de Cachan, 2013, https://tel.archives-ouvertes.fr/tel-00824579.
[36] P.G. Maropoulos, P. Vichare, O. Martin, J. Muelaner, M.D. Summers, A. Kayani, Early design verification of complex assembly variability using a Hybrid – Model Based and Physical Testing – Methodology, CIRP Ann. - Manuf. Technol. 60 (2011) 207–210, https://doi.org/10.1016/j.cirp.2011.03.097.
[37] G. Liu, W. Tang, Y. Ke, Q. Chen, X. Chen, Pre-joining process planning model for a batch of skin – stringer panels based on statistical clearances, Int. J. Adv. Manuf. Technol. 78 (2015) 41–51, https://doi.org/10.1007/s00170-014-6629-2.
[38] K. Xie, J.A. Camelio, L.E. Izquierdo, Part-by-part dimensional error compensation in compliant sheet metal assembly processes, J. Manuf. Syst. 31 (2012) 152–161, https://doi.org/10.1016/j.jmsy.2011.07.005.
[39] G. Liu, H. Huan, Y. Ke, Study on analysis and prediction of riveting assembly variation of aircraft fuselage panel, Int. J. Adv. Manuf. Technol. 75 (2014) 991–1003, https://doi.org/10.1007/s00170-014-6113-z.
[40] A. Pahkamaa, L. Karlsson, J. Pavasson, M. Karlberg, M. Näsström, J. Goldak, A method to improve efficiency in welding simulations for simulation driven design, in: Proc. ASME 2010 Int. Des. Eng. Tech. Conf. Comput. Inf. Eng. Conf., ASME, Montreal, 2010, pp. 1–10.
[41] A. Pahkamaa, K. Wärmefjord, L. Karlsson, R. Söderberg, J. Goldak, Combining variation simulation with welding simulation for prediction of deformation and variation of a final assembly, J. Comput. Inf. Sci. Eng. 12 (2012) 1–6, https://doi.org/10.1115/1.4005720.
[42] M. Préau, P. Hubert, Bonded repairs of composite structures: void formation mechanisms in an adhesive film, in: 17th Eur. Conf. Compos. Mater., Munich, 2016, pp. 26–30.
[43] B. Lindau, S. Lorin, L. Lindkvist, R. Söderberg, Efficient contact modeling in nonrigid variation simulation, J. Comput. Inf. Sci. Eng. 16 (2016) 1–7, https://doi.org/10.1115/1.4032077.
[44] P. Wriggers, Computational Contact Mechanics, second ed., Springer-Verlag, Heidelberg, 2006, pp. 70–71.

2019-05-13

Enhanced bondline thickness analysis for non-rigid airframe structural assemblies

Mato, Pablo Coladas

Elsevier

https://doi.org/10.1016/j.ast.2019.05.024